A reduced-order model for the control of thermoacoustic instabilities in a dump combustor

Quentin Bourny, Camille Sarotte, Aurelien Genot, Didier Theilliol

Symposium on Thermoacoustics in Combustion: Industry meets Academia (SoTiC 2023)
Sept. 11 - Sept. 14, 2023
Zürich, Switzerland

A reduced-order model for the control of thermoacoustic instabilities in a dump combustor

Quentin Bourny[1,2], Camille Sarotte[1],Aurelien Genot[1] and Didier Theilliol[2]

Abstract

Combustion instabilities may develop, due to the formation of vortices at a geometrical change, as a step, which causes flame wrinkling. This may be preponderant for ramjets. In the literature, low-order models for pressure and velocity oscillations have been proposed, in which the oscillations are induced by the coupling between the flame wrinkling and the acoustics. These models have a nonlinear dynamics (kicked oscillator, limit cycle) with a complex frequency spectrum. In order to control the development of thermoacoustic instabilities using these models, they should be written as a state-space representation. However, writing these models under a state-space representation is difficult due to their formulation as kicked oscillators. For this reason, the objective of this paper is to reduce the model to its most simplified form: considering a one-way interaction between the combustor acoustic and the convection of vortices, adopting a deterministic model rather than a stochastic one as proposed by some previous authors. The main contribution of this paper is to propose a reduced-order model, derived from pre-existing models, which is suitable for control. This model is compared to the Nair and Sujith model in this paper and we find satisfactory results: similar spectrum, close amplitude prediction for various operating conditions. This degree of similarity between the models is sufficient in order to develop a model-based control methodology.

Keywords

Reduced-order model, Thermoacoustic instability, Vortex shedding, Dump combustor, Nonlinear state-space representation

Introduction

In combustors, large oscillations of pressure have been observed under certain operating conditions. They are due to thermoacoustic instabilities, which consist of the coupling between the unsteady heat release, the acoustics and the hydrodynamics (Rayleigh 1896; Candel 2002). In practice, combustion instabilities can be responsible for performance degradation or failure. Indeed, the large oscillations of pressure may cause local severe temperature gradients, flame extinction due to flashback, increase in NOx emissions and vibrations (Smith and Zukoski 1985; Candel 2002; Poinsot 2017; Zhao et al. 2018).

To prevent these problems, the control of combustion instabilities have been an active field of research. The methods of control are usually divided between passive and active, depending whether they require or not an external source of energy. If the first ones have been applied to real systems in the rocket industry, they are designed for specific operating conditions and could fail to prevent the development of the instabilities in other conditions (Dowling and Morgans 2005; Zhao et al. 2018). For this reason, the research in active control techniques for the mitigation of combustion instabilities have gained momentum over the last thirty years. If many controllers, sensors or actuators have already been studied, a significant part of the results concerns Rijke tubes (Dowling and Morgans 2005; Zalluhoglu and Olgac 2016; Zhao et al. 2018). However, they are not representative of the complexity of the phenomena which arise in industrial-type combustors. This limitation can be also encountered in certain experimental test-rigs (Poinsot 2017). At the same time, the results obtained from both laboratory test-rigs (Langhorne et al. 1990; McManus et al. 1993; Annaswamy et al. 2000; Campos-Delgado et al. 2003; Morgans and Dowling 2007; Gelbert et al. 2008) and industrial-type gas turbines (Hermann et al. 2000; Riley et al. 2004) showed the potential of active control for the mitigation of thermoacoustic instabilities.

Due to the difficulty to build sufficient databases, most of control approaches published are model-based (McManus et al. 1993; Candel 2002; Dowling and Morgans 2005; Poinsot 2017; Zhao et al. 2018) and therefore require to identify the predominant physical phenomena to select a suitable model. In the special case of ramjet combustors, early experimental investigations have shown the significant role played by the vortex shedding in the development of combustion instabilities (Rogers and Marble 1956; Smith and Zukoski 1985; Poinsot et al. 1987; Schadow and Gutmark 1992; Matveev and Culick 2003). In these combustion systems, the flame is stabilized at a rearward facing step or with a bluff-body (Schadow and Gutmark 1992; Emerson and Lieuwen 2015). The presence of this sudden change in the

[1] DMPE, ONERA, Université Paris-Saclay, F-91123 Palaiseau, France
[2] Université de Lorraine, CNRS, CRAN, F-54000 Nancy, France

Corresponding author:
Quentin Bourny, DMPE, ONERA, Université Paris-Saclay, F-91123 Palaiseau, France
Email: quentin.bourny@onera.fr

geometry causes the formation of vortices at the position of the step, or bluff-body. These vortices induce fluctuations of flame area (Schuller et al. 2020) which lead to heat release rate fluctuations. If these fluctuations are in phase with the acoustic oscillations, combustion instabilities can be observed (Poinsot et al. 1987; Matveev and Culick 2003).

A model, introduced by Matveev & Culick, accounting for the vortex shedding has already been published (Matveev and Culick 2003; Nair and Sujith 2015), but its formulation is not suitable for the control due to the introduction of a stochastic parameter and its formulation as kicked oscillator.

In this paper, the Matveev & Culick model is modified to deduce a simpler model, suitable for control. Nair & Sujith proposed an equivalent formulation of the model, including a modeled noise, and have validated the model on a series of experiment they previously conducted (Nair and Sujith 2013, 2014a,b). In order to validate the proposed model, the same parameters were chosen for the simulations as in Nair and Sujith (2015). In consequence, the formulation from Nair & Sujith is used here.
The first section introduces the initial model, followed by the process conducting to a simplified model, which can be written as a state-space representation, considering the inlet mean flow velocity as the control input of the system. The discretization of the model to account for the sampling of the measurements is presented in the appendix. The validation of the proposed model compared to the original model is presented in the second section. The choice of the control input proposed here was motivated by the comparison with the work of Nair & Sujith (Nair and Sujith 2015).

Vortex Shedding Model

Reference model: Nair and Sujith (2015)

The problem considered in this paper is a backward-facing step followed by a flame attached to a flameholder, positioned at L_c, and a combustor with a length denoted L. This configuration is shown in Figure 1, where $\bar{u}$ indicates the mean flow velocity. In this situation, vortices are formed in the shear layer due to the abrupt change in the geometry ($x = 0$). The vortices impact the flameholder, wrinkling the attached flame. This flame wrinkling causes fluctuations of the heat release rate. When these fluctuations are in phase with the acoustic fluctuations, the thermoacoustic instability arises and potentially destabilizes the flame.

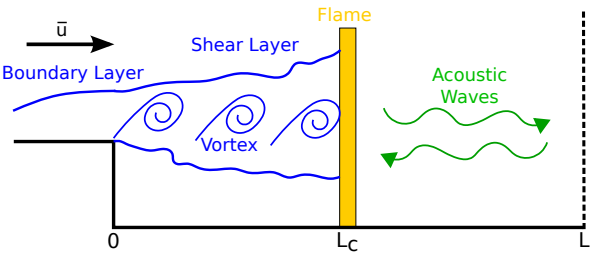

Figure 1. Schematic view of the vortex shedding phenomenon.

The vortex shedding model, proposed first by Matveev & Culick, (Matveev and Culick 2003; Nair and Sujith 2015) was derived under the following assumptions:

- Longitudinal acoustic modes are preponderant. In consequence, the acoustic problem is one-dimensional;
- The effects of flow velocity on the acoustics are negligible;
- The Mach number of the mean flow is assumed to be small;
- The effects of the non-homogeneity due to temperature field are not considered;
- Unsteady heat release rate is restricted to vortices effect;
- Direct combustion noise due to the vortices exceeds the indirect combustion noise. The first one is caused by the vortex-flame interactions as explained previously, while the second one is caused by the acceleration in the outlet nozzle of vorticity or entropy fluctuations (Kings and Bake 2010; Hirschberg et al. 2021);
- Heat release rate fluctuations occur at the moment when a vortex impacts the flameholder;
- During its formation, a vortex does not move significantly compared to its displacement up to the flameholder (or any other impingement point).

Under these assumptions and neglecting the viscous effects, the fluctuations of pressure $p'(x,t)$ and velocity $u'(x,t)$ are governed by the following set of equations as defined in Nair and Sujith (2015):

$$\frac{\partial p'}{\partial t} + \gamma \bar{p} \frac{\partial u'}{\partial x} = (\gamma - 1)\dot{q}' \tag{1}$$

$$\frac{\partial u'}{\partial t} + \frac{1}{\bar{\rho}} \frac{\partial p'}{\partial x} = 0 \tag{2}$$

with the heat release rate fluctuations $\dot{q}'(x,t)$ modelled as:

$$\dot{q}'(x,t) = \beta \sum_j \Gamma_j \delta(t - t_j)\delta(x - L_c) \tag{3}$$

where j refers to the j-th vortex (Matveev and Culick 2003), Γ_j is the vorticity of the vortex j and t_j is the instant of the j-th vortex impact with the flameholder located at the position L_c. $\bar{p}$ is the mean static pressure. β is a constant relating the heat release rate fluctuations and the vortex impingement to the flameholder (Nair and Sujith 2015).
Using the Galerkin's decomposition and assuming the system behaves as a closed-open duct, the fluctuations of pressure and velocity in the combustor can be expanded into N basis functions:

$$p'(x,t) = \bar{p} \sum_{n=1}^{N} \frac{\dot{\eta}_n(t)}{\omega_n} \cos(k_n x) \tag{4}$$

$$u'(x,t) = \frac{\bar{a}}{\gamma} \sum_{n=1}^{N} \eta_n(t) \sin(k_n x) \tag{5}$$

where the index n denotes the values related to the n-th time-varying amplitude: η_n, whose derivative is denoted $\dot{\eta}_n$. $\bar{a}$ is the mean sound velocity. The angular wavenumber k_n and angular frequency ω_n are related by the following dispersion relation:

$$k_n = \frac{\omega_n}{\bar{a}} \tag{6}$$

The angular wavenumber is given by:

$$k_n = \frac{(2n-1)\pi}{2L} \tag{7}$$

By substituting these expansions into equation (1) and projecting on the basis functions, a set of N second-order ordinary differential equations is deduced:

$$\ddot{\eta}_n + \xi_n \dot{\eta}_n + \omega_n^2 \eta_n = c\omega_n \cos(k_n L_c) \sum_j \Gamma_j \delta(t - t_j) \tag{8}$$

where $\delta(\cdot)$ is the Dirac distribution, $c = 2(\gamma-1)\beta/L\bar{p}$ and $\xi_n/\xi_1 = (2n-1)^2$.
The damping term $\xi_n \dot{\eta}_n$ was introduced ad hoc to account for the acoustic losses (Matveev and Culick 2003; Nair and Sujith 2015).
The convection of the vortices from the step is modelled as:

$$\frac{dx_j}{dt} = \alpha \bar{u} + u'(x_j, t) \tag{9}$$

where $\bar{u}$ is the mean flow velocity, x_j is the position of the j-th vortex and α follows a Gaussian distribution in order to account for the variability of the vortex characteristics and the influence of turbulence (Nair and Sujith 2015).
The vortex formation is controlled by the rate of change of circulation at the step via the equation:

$$\frac{d\Gamma}{dt} = \frac{1}{2}\bar{u}^2 \tag{10}$$

When the circulation exceeds a critical value Γ_{crit}, a new vortex is formed. This critical value is obtained with the following relation:

$$\Gamma_{crit} = \frac{\bar{u}d}{2St} \tag{11}$$

where St denotes the Strouhal number for the step of height d and the mean flow velocity $\bar{u}$ (Matveev and Culick 2003; Nair and Sujith 2015).

From the vortex shedding model (Eq. (8)) and introducing the vector $X = (\eta_1, \cdots, \eta_N, \dot{\eta}_1, \cdots, \dot{\eta}_N)^T$, the set of equations governing the amplitudes is given by the following state space equation:

$$\dot{X} = AX + E\mathcal{S}(X, t, x_j, \bar{u}) \tag{12}$$

where $E\mathcal{S}(X, t, x_j, \bar{u})$ corresponds to the source term due to vortex combustion with:

$$\mathcal{S}(X, t, x_j, \bar{u}) = \sum_j \Gamma_j \delta(t - t_j) \tag{13}$$

and the matrices A and E are given by:

$$A = \begin{pmatrix} 0_{N,N} & I_N \\ -\Omega^2 & -\Xi \end{pmatrix} \tag{14}$$

with $\Omega = diag(\omega_1, \cdots, \omega_N)$, $\Xi = diag(\xi_1, \cdots, \xi_N)$ and $E = (0_{N,1}, c\omega_1 \cos(k_1 L_C), \cdots, c\omega_N \cos(k_N L_c))^T$. As shown by the equation 9, the instant of impact t_j depends on the mean inlet flow velocity $\bar{u}$ and the acoustic fluctuations of flow velocity u' at the vortex position x_j and for the state vector X, giving the dependency of the source term on X ,x_j and $\bar{u}$. The main issue in this state-space representation is the complexity to explicitly write the source term depending of the state vector X and the mean flow velocity $\bar{u}$. In the following subsection, simplifications of the vortex shedding model are proposed and the motivations for these simplifications are presented.

Motivations and proposed reduced-order model

Some parameters, like the Strouhal number or the coefficient β which play a preponderant role in the model, are obtained empirically, involving a certain level of uncertainty. This involves a certain level of robustness with respect to the model parameters is necessary for a controller based on this model.
It is chosen in this paper to use a discrete model for convenience.
Another reason limits the use of the original model for a model-based control methodology: the introduction of a stochastic value for the coefficient α. The choice of a stochastic rather than deterministic value for the coefficient α was motivated by the influence of turbulence and the variability of vortex size (Nair and Sujith 2015). Within the scope of developing a control methodology, these can be considered as disturbances of the nominal system, i.e. the system with a constant α. They are accessible via the measurements of the fluctuations of acoustic pressure, even though it involves appropriate choices for the sampling period, the sensor position and to deal with the measurement noise.

In summary, the model shall be discrete and explicitly dependent of the inlet mean flow velocity, $\bar{u}$, considered as the control input in this paper. Uncertainties due to the modelling or the parameters shall be accessible as an additive perturbation to the model. The main objectives of this model reduction are to keep the dominant frequencies, the dependence of the acoustics on the inlet flow velocity and to correctly predict the level of the acoustic pressure oscillations. The correct prediction of the dominant frequencies is necessary to capture the transition to the combustion instability, which occurs when hydrodynamic and acoustic frequencies are commensurate (Nair and Sujith 2015). Moreover, the model was derived under the assumption of quasi-steady inlet flow velocity, thus its variation must be slow enough to be negligible with respect to the dominant frequencies of the system.
For these reasons, it is proposed to simplify the equation (9) by choosing α equal to a constant α_0 and neglecting the velocity fluctuations $u'(x_j, t)$, which represents an additional source of fluctuations in vortex convection velocity. These simplifications give the following equation for the convection of the vortices:

$$\frac{dx_j}{dt} = \alpha_0 \bar{u} \tag{15}$$

As depicted in Figure 2, the coupling between the flame, the acoustics and the hydrodynamics is modelled in the original model as a one-way coupling between the transport of the vortices, the flame wrinkling and the acoustics. The reduction to the proposed model translates into neglecting the influence of the acoustics on the transport of the vortices (illustrated by the red cross).

Considering these simplifications, the model is schematically formulated in the discrete form with Δt the time step and at the instants $t_k = k\Delta t$:

$$X_{k+1} = \tilde{A}_k X_k + \tilde{E} S_k^h \tag{16}$$

where $\tilde{A}_k$ and $\tilde{E}$ are matrices, X_k is the state vector, u_k the inlet mean flow velocity and S_k^h a certain function of

u_k given by Eq. (35), all written at the instant t_k. The exact expression of each term depends on the discretization scheme and is given in the appendix.

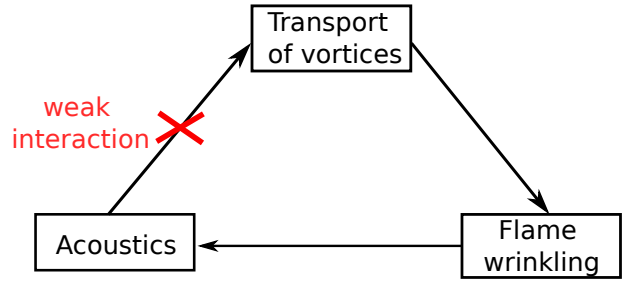

Figure 2. Schematic representation of the coupling between the transport of vortices, the acoustics and the heat release rate fluctuations in the original model and in the proposed model

Validation of the proposed model

This section presents the validation process of the previously introduced model by comparison with the original model.

Parameters and numerical implementation

In order to compare the simplified and the original models, the same numerical parameters as in Nair and Sujith (2015) are used, excepted the time step Δt, reduced from $5 \cdot 10^{-5}$ s to $1 \cdot 10^{-5}$ s since the discretization schemes are different. The numerical parameters are summarized in the table 1.

Two inlet velocities have been considered: 8 and 9 m/s corresponding to two different dynamics: intermittent (chaotic) regime and self-sustained thermoacoustic instability respectively (Nair and Sujith 2015).

Parameter	Value
Δt	$1 \cdot 10^{-5}$ s
L	0.7 m
L_c	0.05 m
d	0.025 m
N	10
$\bar{p}$	10^5 Pa
$\bar{a}$	700 m/s
γ	1.4
St	0.35
ξ_1	29 s^{-1}
c	$6 \cdot 10^{-3}$ $m^{-2} \cdot s$

Table 1. Parameters used for the model validation, based on (Nair and Sujith 2015)

The numerical scheme used for the original model is the pre-implemented function ODEINT available in the scipy.integrate library, based on the LSODA solver, an adaptive order and adaptive step method (Petzold 1983; Hindmarsh 1983). For the proposed model, the trapezoidal rule was used. A discussion about the influence of the discretization scheme is detailed in the appendix.

Comparison of the source term

The source term $\mathcal{S} = \sum_j \Gamma_j \delta(t - t_j)$ in Eq (8) is plotted over time in the Figure 3 for the two models. The source term for the "original model" is obtained with Eq. (9), while the source term for the "proposed model" is obtained with Eq. (15). In Figure 3, it is observed that the proposed model is a strictly periodic Dirac comb, while the original one is only a quasi-periodic pulse train causing low random shifts in time.

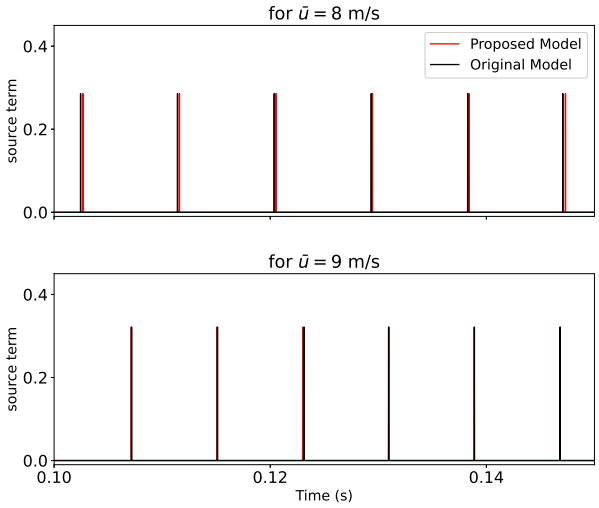

Figure 3. Comparison of the source term, $\mathcal{S} = \sum_j \Gamma_j \delta(t - t_j)$, obtained with the proposed and original models for the two inlet flow velocities

The differences are caused by the influence on the vortex convection velocity of the acoustic flow velocity and of the random choice of α. Both terms can increase or reduce the convection velocity and in consequence, the two models exhibit a regular synchronization of the source term, as shown in Table 2 in which the differences are small between the two models. For this reason, the amplitude spectrum of the source should present similar eigenfrequencies but differs between the models in terms of low-amplitude components. Figure 4 shows the amplitude spectrum for the two different inlet mean flow velocities, i.e. 8 and 9 m/s, obtained with the fast Fourier Transform of the source term. This figure exposes that the dominant frequencies are identical for both models, proving the proposed model is able to predict the heat periodic release rate fluctuations due to the vortex shedding in a similar manner as the original model.

To quantitatively compare the source term obtained with the two models, the instant of vortex impacts predicted by both models were computed. Table 2 summarizes the average, minimum and maximum for the time series given by:

$$\frac{t_j^{orig} - t_j^{prop}}{\Gamma_{crit}/(0.5\bar{u}^2)} \tag{17}$$

where $\Gamma_{crit}/(0.5\bar{u}^2)$ represents an averaged period between two impacts of a vortex on the flameholder. The original model is indicated by the exponent "orig", while the proposed model is indicated by "prop". The amplitude of the source term is identical with the original model by construction of the proposed model. It proves the quasi-periodicity of the original model and shows both models

predict similar instants for the vortex impingement on the flameholder.

$\bar{u}$ (m/s)	Maximum (%)	Minimum (%)	Average (%)
8	0.34	-3.81	-2.16
9	2.52	-3.53	0.11

Table 2. Maximum, minimum and average of the adimensional difference between the instant of impact, t_j, predicted by both models given by Eq. (17)

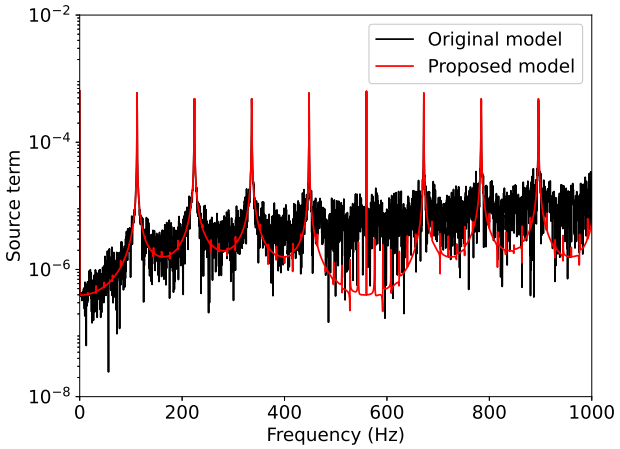

(a) $\bar{u} = 8$ m/s

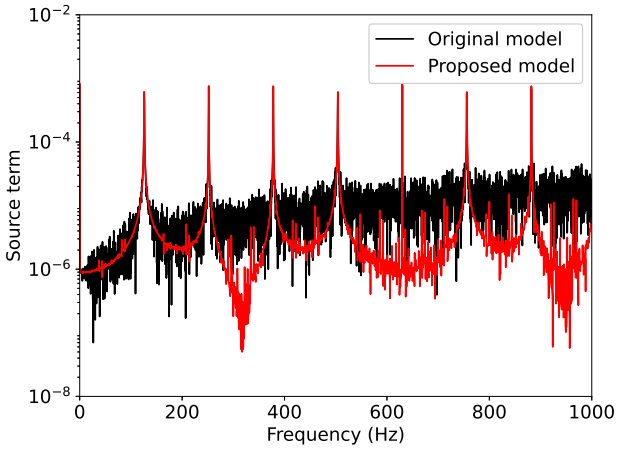

(b) $\bar{u} = 9$ m/s

Figure 4. Amplitude spectrum of the source term $\mathcal{S} = \sum_j \Gamma_j \delta(t - t_j)$ for the two inlet flow velocities

It has been shown that the proposed model predicts a similar source term as the original model in terms of amplitude and dominant frequencies. The observed differences were due to random shifts due to the stochastic parameter α. In the next subsection, the impact of these differences and similarities is analysed with the acoustic pressure oscillations.

Comparison of the acoustic pressure oscillations

A characteristic feature of the thermoacoustic instabilities is the development of a limit cycles with large amplitudes of pressure oscillations. For this reason, the oscillations of pressure predicted by the original and proposed models are compared in this subsection for two regimes: intermittency and thermoacoustic instability.

Figure 5 displays the time evolution of acoustic pressure fluctuations predicted by the proposed and the original models (Eq. (4) with respectively (15) and (9)). It shows, with Table 3, that the amplitude of the oscillation of acoustic pressure is correctly predicted by the proposed model for both the intermittent regime and the instability regime.

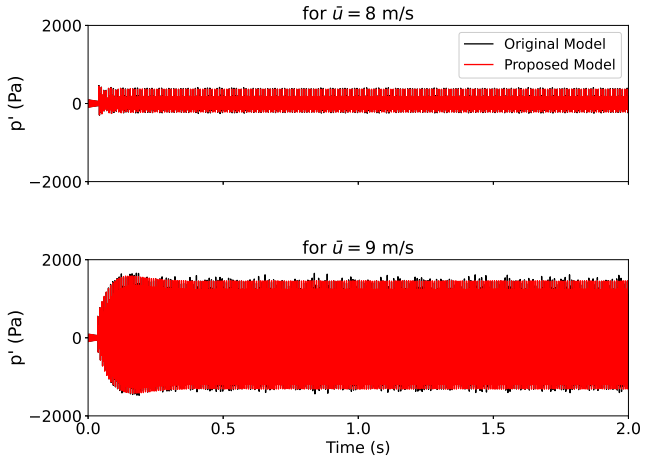

Figure 5. Acoustic pressure p' at the position $x = 0.09$ m for the two inlet flow velocities

$\bar{u}$	$\max(p'_{orig})$	$\max(p'_{prop})$
8 m/s	446.9 Pa	443.2 Pa
9 m/s	1707 Pa	1583 Pa

Table 3. Maximal error in acoustic pressure oscillations p' relative to the original model for both regime

The difference yields as with the source term in the strict periodicity of the proposed model compared to the quasi-periodicity of the original model, causing a random variability in the amplitude for the latter. To confirm this observation, the acoustic pressure fluctuations were plotted for a smaller interval as shown in Figure 6. The periodic pattern given by the two models are similar. Since the phase of source term is randomly changed, the pressure discontinuity induced by the impact of a vortex presents a random phasing, explaining the two signals regularly desynchronize. This observation is confirmed by the amplitude spectrum of acoustic pressure (at $x = 0.09$ m) which presents the same dominant frequencies in the Figure 7. The general envelope of the amplitude spectrum are qualitatively identical. The main difference is the acoustic peak, which is less intense for the proposed model than for the original model.

It was observed that the acoustic peak was less intense with larger time steps for $\bar{u} = 8$ m/s. In addition, the amplitude spectrum of the source term was observed to reach lower levels for larger time step, excepted the peaks associated to the hydrodynamic frequencies. These observations are likely due to the numerical scheme, which

filters the less dominant frequencies in the source term spectrum for larger time steps, and to the assumption of negligible influence of the acoustic flow velocity on the vortex convection. It indicates the time step shall be carefully chosen as a compromise between the computational cost and the ability to capture the dominant frequencies with a sufficient precision. The second explanation is illustrated by Figure 8, which depicts the amplitude spectrum of the acoustic flow velocity at the position $x = 0.09$ m. The amplitude spectrum for the oscillations of acoustic flow velocity exhibits the hydrodynamic and acoustic frequencies, the latter being not fully captured. The absence of this influence on the vortex convection may explain the lower amplitude of the "acoustic peaks" predicted by the proposed model compared to the original one, for $\bar{u} = 8$ m/s. This difference is not observed when the hydrodynamic and acoustic frequencies are in-phase, when the instability occurs.

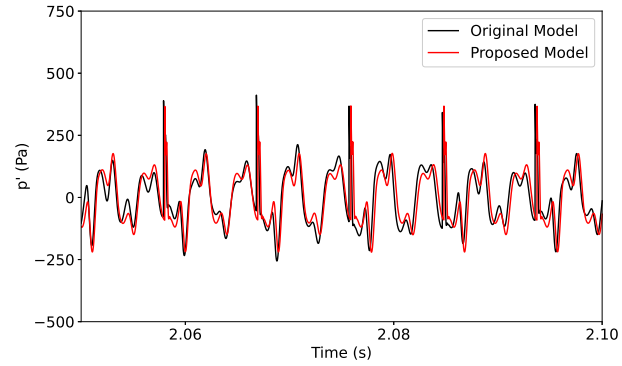

(a) $\bar{u} = 8$ m/s

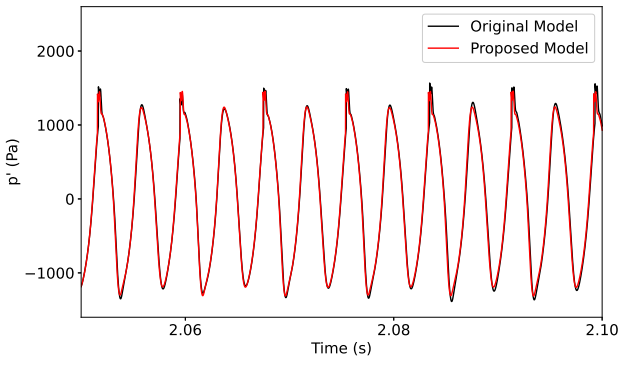

(b) $\bar{u} = 9$ m/s

Figure 6. Acoustic pressure p' at the position $x = 0.09$ m for the two inlet flow velocities, zoomed between 2.06 and 2.10 seconds

Figure 9 indicates the amplitude of the acoustic pressure in the x-position-frequency plane. It extends the previous analysis to all the position in the combustor. The pressure nodes are identically positioned between the two model, the main difference concerning the amplitude of the acoustic peaks, as previously observed in the figures 7 and 8.

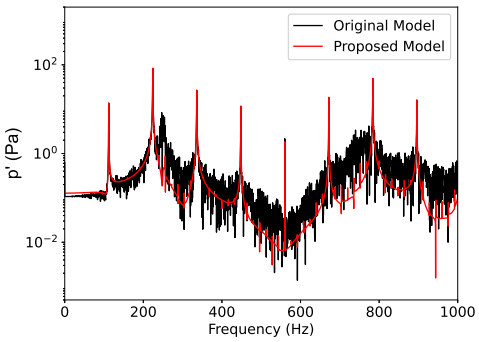

(a) $\bar{u} = 8$ m/s

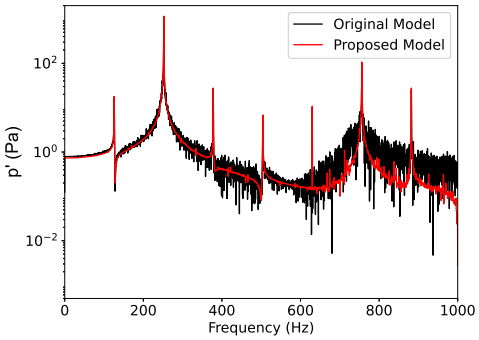

(b) $\bar{u} = 9$ m/s

Figure 7. Amplitude spectrum of the acoustic pressure p' at the position $x = 0.09$ m

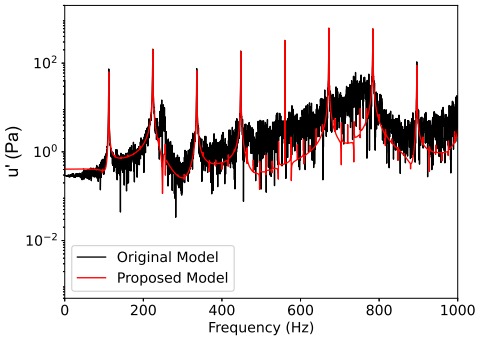

(a) $\bar{u} = 8$ m/s

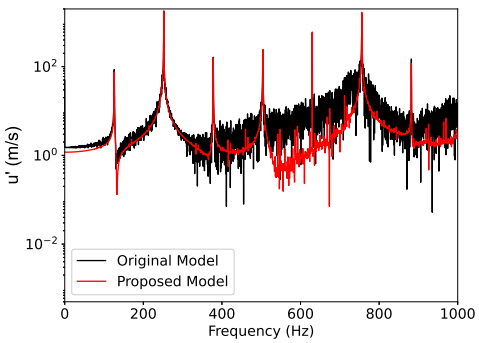

(b) $\bar{u} = 9$ m/s

Figure 8. Amplitude spectrum of the acoustic flow velocity u' at the position $x = 0.09$ m

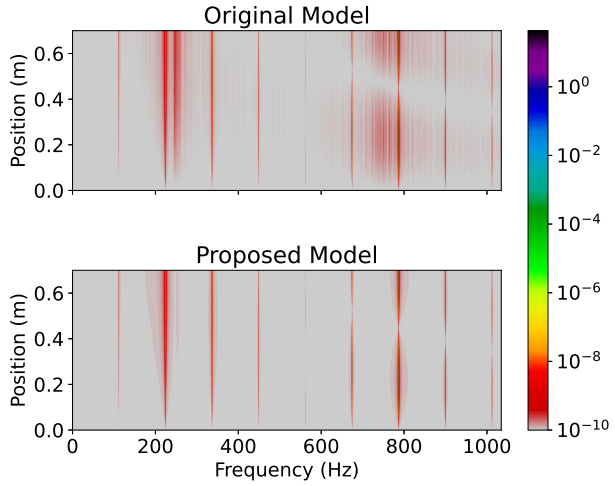

(a) $\bar{u} = 8$ m/s

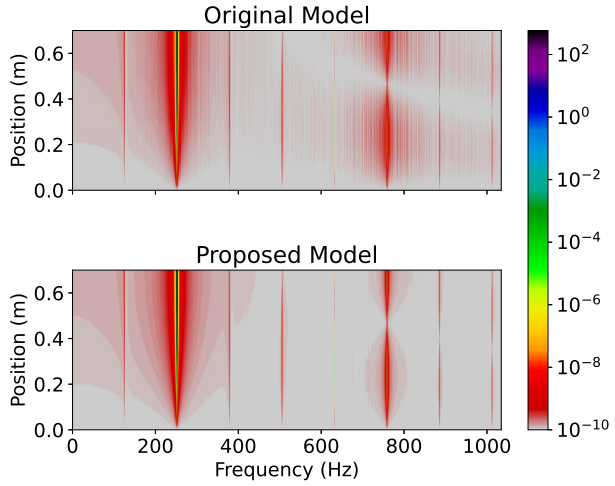

(b) $\bar{u} = 9$ m/s

Figure 9. Amplitude spectrum of the acoustic pressure p' against frequency and position in the combustor

Conclusion and Perspectives

In order to design a controller, a published model of vortex shedding was simplified by eliminating the dependency of the vortex convection process to a stochastic parameter and to the acoustic flow velocity. The first simplification consists of transforming a model - in which an uncertainty of imposed level, non-linearly intervened in the model and is difficult to estimate - to a model for which the uncertainty can be estimated as an additive perturbation.

The simplified model reproduced the characteristic frequencies due to the hydrodynamics and the amplitude of the acoustic pressure. In addition, the periodicity of the heat release rate fluctuations due to the vortices was also correctly captured by the proposed simplified model.

The formulation proposed of the model can account for the variability of a inlet mean flow velocity under the assumption of quasi-steadiness of this change.

From this simplified model, a state-space equation could be derived and modern optimal design techniques, as model predictive control, can be expected to be synthesized to control a dump combustor destabilized by the vortex shedding.

Acknowledgements

The authors would like to gratefully acknowledge ONERA and French Defense Ministry - Defense Innovation Agency for their financial support. In addition, the authors are grateful to M. Voisine and A. Leroy from DGA for their support.

References

Annaswamy AM, Fleifil M, Rumsey JW, Prasanth R, Hathout J-P and Ghoniem AF (2000) Thermoacoustic instability: model-based optimal control designs and experimental validation, *IEEE Transactions on Control Systems Technology*, vol. 8, no. 6, pp. 905-918

Candel S (2002) Combustion dynamics and control: Progress and challenges, *Proceedings of the Combustion Institute*, vol. 29, no. 1, pp. 1-28

Campos-Delgado DU, Schuermans BBH, Zhou K, Paschereit CO, Gallestey EA and Poncet A (2003) Thermoacoustic instabilities: modeling and control, *IEEE Transactions on Control System Technology*, vol. 11, no. 4, pp. 429-447

Dowling AP and Morgans AS (2005) Feedback Control of Combustion Oscillations, *Annual Review of Fluid Mechanics*, vol. 37, pp. 151-182

Emerson B and Lieuwen T (2015) Dynamics of harmonically excited, reacting bluff body wakes near the global hydrodynamic stability boundary, *Journal of Fluid Mechanics*, vol. 779, pp. 716-750

Gelbert G, Moeck J P, Bothien MR, King R and Paschereit CO (2008) Model Predictive Control of Thermoacoustic Instabilities in a Swirl-Stabilized Combustor, *46th AIAA Aerospace Sciences Meeting and Exhibit*, Reno, NV, USA, 7-10 January 2008

Hermann J, Orthmann A, Hoffmann S and Berenbrink P (2000) Combination of Active Instability Control and Passive Measures to Prevent Combustion Instabilities in a 260MW Heavy Duty Gas Turbine, *RTO AVT Symposium* on *Active Control Technology for Enhanced Performance Operational Capabilities of Military Aircraft, Land Vehicles and Sea Vehicles*, Braunschweig, Germany, 8-11 May 2000

Hindmarsh AC (1983) A Systematized Collection of ODE Solvers, in *Scientific Computing*, R.S. Stepleman et al. (Eds.), North-Holland, Amsterdam, pp. 55-64

Hirschberg L, Hulshoff SJ and Bake F (2021) Sound production due to Swirl-Nozzle interaction: Model-based analysis of experiments, *AIAA Journal*, vol. 59, no. 4, pp. 1269-1276

Kings N and Bake F (2010) Indirect combustion noise: noise generation by accelerated vorticity in a nozzle flow, *International journal of spray and combustion dynamics*, vol. 2, no. 3, pp. 253-266

Langhorne P J, Dowling AP and Hooper N (1990) Practical active control system for combustion oscillations, *Journal of Propulsion and Power*, vol. 6, no. 3, pp. 324-333

Matveev KI and Culick FEC (2003) A model for combustion instability involving vortex shedding, *Combustion Science and Technology*, vol. 175, no. 6, pp. 1059-1083

McManus KR, Poinsot T and Candel S (1993) A review of active control of combustion instabilities, *Progress in Energy and Combustion Science*, vol. 19, no. 1, pp. 1-29

Morgans AS and Dowling AP (2007) Model-based control of combustion instabilities, *Journal of Sound and Vibration*, vol.

299, no. 1-2, pp. 261-282

Nair V, Thampi G, Karuppusamy S, Gopalan S and Sujith RI (2013) Loss of chaos in combustion noise as a precursor of impending combustion instability, *International journal of spray and combustion dynamics*, vol. 5, no. 4, pp. 273-290

Nair V and Sujith RI (2014) Multifractality in combustion noise: predicting an impending combustion instability, *Journal of Fluid Mechanics*, vol. 747, pp. 635-655

Nair V, Thampi G and Sujith RI (2014) Intermittency route to thermoacoustic instability in turbulent combustors, *Journal of Fluid Mechanics*, vol. 756, pp. 470-487

Nair V and Sujith RI (2015) A reduced-order model for the onset of combustion instability: Physical mechanisms for intermittency and precursors, *Proceedings of the Combustion Institute*, vol. 35, pp. 3193-3200

Paschereit CO, Gutmark E and Weisenstein W (1998) Control of thermoacoustic instabilities and emissions in an industrial-type gas-turbine combustor, *27th Symposium (International) on Combustion*, vol. 27, no. 2, pp. 1817-1824

Petzold L (1983) Automatic Selection of Methods for Solving Stiff and Nonstiff Systems of Ordinary Differential Equations, *SIAM Journal on Scientific and Statistical Computing*, vol. 4, no. 1, pp. 136-148

Poinsot T, Trouvé A, Veynante D, Candel S and Esposito E (1987) Vortex-driven acoustically coupled combustion instabilities, *Journal of Fluid Mechanics*, vol. 177, pp. 265-292

Poinsot T (2017) Prediction and control of combustion instabilities in real engines, *Proceedings of the Combustion Institute*, vol. 36, pp. 1-28

Rayleigh L (1896) *The Theory of Sound*. London: MacMillan, 2nd edition, Vol. 2, pp 224–234

Riley AJ, Park S, Dowling AP, Evesque S and Annaswamy AM (2004) Advanced Closed-Loop Control on an Atmospheric Gaseous Lean-Premixed Combustion, ASME *Journal of Engineering for Gas Turbines and Power*, vol. 126, no. 4, pp. 708-716

Rogers DE and Marble FE (1956) A Mechanism for High-Frequency Oscillation in Ramjet Combustors and Afterburners, *Journal of Jet Propulsion*, vol. 26, no. 6, pp. 456-462

Schadow KC and Gutmark E (1992) Combustion instability related to vortex shedding in dump combustors and their passive control, *Progress in Energy and Combustion*, vol. 18, no. 2, pp. 117-132

Schuller T, Poinsot T and Candel S (2020) Dynamics and control of premixed combustion systems based on flame transfer and describing functions, *Journal of Fluid Mechanics*, vol. 894, P1

Smith DA and Zukoski EE (1995) Combustion Instability Sustained by Unsteady Vortex Combustion, *AIAA/SAE/ASME/ASEE 21st Joint Propulsion Conference*, Monterey, CA, USA, 8-10 July 1985

Yu K, Trouvé A and Daily J (1991) Low-frequency pressure oscillations in a model ramjet combustor, *Journal of Fluid Mechanics*, vol. 232, pp. 47-72

Zalluhoglu U and Olgac N (2016) Deployment of Time-Delayed Integral Control for Suppressing Thermoacoustic Instabilities, *Journal of Guidance, Control and Dynamics*, vol. 39, no. 10, pp. 2284-2296

Zhao D, Lu Z, Zhao H, Li XY, Wang B and Liu P (2018) A review of active control approaches in stabilizing combustion systems in aerospace industry, *Progress in Aerospace Sciences*, vol. 97, pp. 35-60

Appendix: detailed derivation of the proposed model

This appendix aims to propose a detailed derivation of the model presented in this paper. For this reason, it starts with a discussion about the choice of an appropriate discretization scheme for the integrated equations. It shows the trapezoidal rule is sufficient. This section ends with a detailed derivation of the source term depending on an slow time-varying inlet mean flow velocity.

Choice of the discretization scheme

Let introduce $t_k = k\Delta t$ and $t_{k+1} = (k+1)\Delta t$ two consecutive instants and Δt the discretization period. By assuming $\bar{u}$ is constant between two instants and denoting u_k its value, the integration between t_k and t_{k+1} of the equation (12) gives the following equation:

$$X_{k+1} = X_k + A\int_{t_k}^{t_{k+1}} X(t)dt + E\int_{t_k}^{t_{k+1}} \mathcal{S}(X_k, t, x_j, u_k)dt \tag{18}$$

with X_k denoting the state vector at the instant t_k.

In order to choose an appropriate approximation for the integral $\int_{t_k}^{t_{k+1}} X(t)dt$, a simple configuration was considered. In absence of source term, the problem can be solved analytically. This process is equivalent to the solving method usually used for kicked oscillators: solving the oscillator equation without the source term and if necessary applying a jump condition to include the source term (Matveev and Culick 2003; Nair and Sujith 2015). In consequence, the modelling process can be divided into two steps: to find an appropriate time discretization for the oscillator equation and to model the impact of the source term on the solution. The first step is dealt in this section, the second step is the topic of the next section.

Considering the first amplitude and an initial state $(0.001, 0)$, the solutions obtained analytically, with the Python pre-implemented function ODEINT, with the trapezoidal rule, with the implicit and explicit Euler methods have been computed and are compared in Figure 10 and Table 4. The errors in Table 4 were computed as:

$$err(\eta) = \frac{|\eta^{analyt} - \eta^{scheme}|}{0.001} \tag{19}$$

$$err(\dot{\eta}) = \frac{|\dot{\eta}^{analyt} - \dot{\eta}^{scheme}|}{1.5} \tag{20}$$

where the analytical solution stands for "analyt" and the solution associated to a certain numerical scheme "scheme".

Integration scheme	$\max\{err(\eta)\}$	$\max\{err(\dot{\eta})\}$
ODEINT	0.91%	0.0001%
Trapezoidal rule	0.91%	0.0001%
Euler implicit	22.31%	0.13%

Table 4. Maximal error on the amplitude and its derivative for different numerical integration scheme, for the initial condition $\eta_1(t=0) = 0.001$ and $\dot{\eta}_1(t=0) = 0$

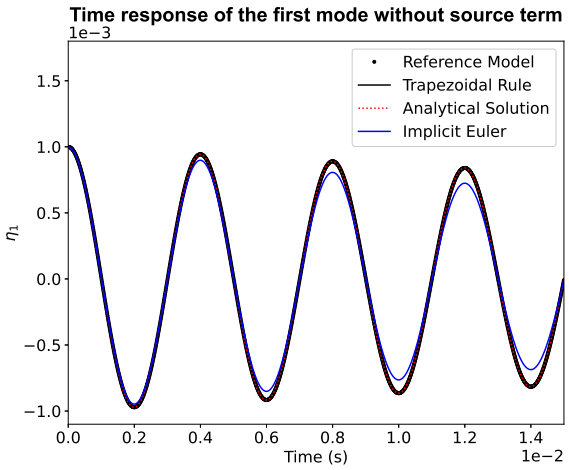

Figure 10. Comparison of the time response of the first amplitude for the initial conditions $\eta_1(t=0) = 0.001$ and $\dot{\eta}_1(t=0) = 0$

The results showed the use of the implicit Euler method was likely to overdamp the time response. It was observed that the numerical solution diverges for the explicit Euler method. In terms of error, the trapezoidal scheme gave an acceptable match with the analytical solution and shall be chosen for the discretization.

Simplified modelling of the vortex shedding

Given the previous subsection, the trapezoidal rule was proved to be sufficient for the modelling. Using the trapezoidal rule to approximate in Eq. (18), the state equation could be recast as:

$$X_{k+1} = \tilde{A}X_k + \tilde{E}\int_{t_k}^{t_{k+1}} \mathcal{S}(X_k, t, x_j, u_k)dt \tag{21}$$

with:

$$\tilde{A} = \left(I_{2N} - \frac{\Delta t}{2}A\right)^{-1}\left(I_{2N} + \frac{\Delta t}{2}A\right) \tag{22}$$

$$\tilde{E} = \left(I_{2N} - \frac{\Delta t}{2}A\right)^{-1}E \tag{23}$$

In the equation (21), one term was still not explicitly discretized: $\int_{t_k}^{t_{k+1}} \mathcal{S}(X_k, t, x_j, \bar{u}(t))dt$. The objective of this section is to propose an explicit expression for this integral.

At the step, the circulation increases up to a critical value, causing the formation of a vortex j characterized by its position $x_j(t)$ and its vorticity, assumed to be constant over time, Γ_j. The increase of circulation is controlled by the inlet mean flow velocity $\bar{u}$. This vortex is then convected until it reaches an obstacle, here a flameholder, at a certain time denoted t_j. This impact can occur during the same interval as the vortex formation or afterwards. At the instant of the vortex impact on the flameholder, the attached flame is wrinkled. The flame wrinkling causes fluctuations of heat release rate, which modify the acoustic fluctuations. The process is then repeated for each vortex and each discrete time.

By introducing a distinction among the vortices formed during an interval between the ones which impact the flameholder during the same interval and the others which impact in a subsequent interval, the source term can be expressed as:

$$\int_{t_k}^{t_{k+1}} \mathcal{S}(X_k, t, x_j, u_k)dt = S_k^c + S_k^h \tag{24}$$

As depicted in Figure 11, S_k^c corresponds to the vortices which impact the flameholder during the same interval as they are created. S_k^h accounts for the vortices which are still convected at the end of their formation interval and they shall be convected at each time step until they reach the flameholder. However, in practice, the time step is smaller than the convection time and the period between the formation of two consecutive vortices. This constraint is necessary to ensure the model can capture the physical predominant frequencies. In consequence, the term S_k^c in the equation (24) is neglected, giving the following expression for the source term:

$$\int_{t_k}^{t_{k+1}} \mathcal{S}(X_k, t, x_j, u_k)dt = S_k^h \tag{25}$$

Following the previous discussion, the number of vortices formed during an interval is first deduced. Next, the source term S_k^h is deduced.

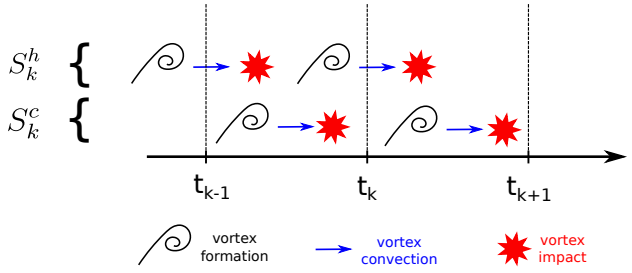

Figure 11. Schematic representation of the distinction used in Eq. (24)

The source term depends of the position of the vortices, their vorticity and their number. The integration of the equation (10) is not straightforward, since the circulation shall be reduced by the circulation used to create new vortices. To start the derivation of the model, the number of vortices formed during a certain interval is obtained. It depends on the circulation at each instant. For this reason, the circulation available during an interval to form vortices is first expressed before giving the relation to compute the total number of vortices formed during an interval, denoted N_k^v.

Let Γ_{k+1}^r denote the remaining circulation after the creation of the new vortices at the end of the interval $[t_k, t_{k+1}]$, i.e. at the instant t_{k+1}. The circulation available between t_k and t_{k+1}, denoted Γ_k^a, is then the sum of the remaining circulation at t_k with the circulation created at the step, i.e.

$$\Gamma_k^a = \Gamma_k^r + \frac{1}{2}\Delta t u_k^2 \tag{26}$$

where u_k denotes the inlet mean flow velocity during the interval $[t_k, t_{k+1}]$.

Given the circulation available during the interval, the number of vortices formed during the same interval, denoted

N_k^v, is obtained with the following equation:

$$N_k^v = \left\lfloor \frac{\Gamma_k^a}{\Gamma_{crit}(k)} \right\rfloor \tag{27}$$

with $\Gamma_{crit}(k)$ the critical value of circulation during the interval $[t_k, t_{k+1}]$.
From this definition, it is then possible to define the remaining circulation at a given instant:

$$\Gamma_{k+1}^r = \Gamma_k^r + \frac{1}{2}\Delta t u_k^2 - N_k^v \Gamma_{crit}(k) \tag{28}$$

where $N_k^v \Gamma_{crit}(k)$ corresponds to the circulation consumed by the formation of the vortices.
The vortices, formed during the interval $[t_k, t_{k+1}]$, impact the flameholder during a next interval, depending of the convection velocity and the time step of discretization.

S_k^h, the source term due to the vortices impacting the flameholder but formed at a previous interval, is the last term to model in order to achieve a complete discrete formulation of the Matveev and Culick model. In what follows, the position of each vortex is expressed as a function of the inlet mean velocity and the circulation. From the knowledge of the position of every vortex, it is possible to express their contribution to the source term.
Let $x_m^K(k)$ denote the position of the m-th vortex at the instant t_k and formed during the interval $[t_K, t_{K+1}]$. Integrating the convection equation (9) and assuming the acoustic fluctuations of velocity have a negligible influence on convection, the position of the vortex is given by:

$$x_m^K(k+1) = x_m^K(k) + \alpha_0 u_k \Delta t \tag{29}$$

By induction, the position can be expressed as a function of the mean flow velocity:

$$x_m^K(k) = \sum_{l=1}^{k-1-K} \alpha_0 u_{K+l} \Delta t + x_m^K(K+1) \tag{30}$$

$x_m^K(K+1)$ corresponds to the position of the vortex m formed during $[t_K, t_{K+1}]$ at the instant t_{K+1}. If the instant of its formation is denoted t_m^K, its position is:

$$x_m^K(K+1) = \alpha_0 u_K (t_{K+1} - t_m^K) \tag{31}$$

The last vortex formed during the previous interval and impacting the flameholder during the considered interval impacts the flameholder at the instant $t_K - \Gamma_K^r/(u_K^2/2)$. A vortex is periodically formed with a period of $\Gamma_{crit}(K)/(0.5u_K^2)$. The instant of formation t_m^K is thus given by the following equation:

$$t_m^K = t_K - \frac{\Gamma_K^r}{u_K^2/2} + m\frac{\Gamma_{crit}(K)}{u_K^2/2} \tag{32}$$

Substituting into the equation (31) gives the initial position of the m-th vortex, formed at the interval $[t_K, t_{K+1}]$:

$$x_m^K(K+1) = \alpha_0 u_K \left(\Delta t + \frac{2\Gamma_{crit}(K)}{u_K^2} \left\{ m - \frac{\Gamma_K^r}{\Gamma_{crit}(K)} \right\} \right) \tag{33}$$

Since the position of every vortex is fully known, the only relation still required is between the vortex position and the source term S_k^h.
The influence of a vortex over the combustion is limited to a certain time interval. To indicate whether a vortex m, formed at the interval K, impacts the flameholder during the interval $[t_k, t_{k+1}]$, let $\mathbb{1}_{m,K}(k)$ be the indicator function given by:

$$\mathbb{1}_{m,K}(k) = \mathcal{U}(x_m^K(k+1) - L_c) - \mathcal{U}(x_m^K(k) - L_c) \tag{34}$$

with $\mathcal{U}(\cdot)$ the Heaviside function. Using this indicator function to indicate the vortices which impact the flameholder at the considered interval, the source term S_k^h can be expressed as:

$$S_k^h = \sum_{K=0}^{k-1} \Gamma_{crit}(K) \sum_{m=1}^{N_K} \mathbb{1}_{m,K}(k) \tag{35}$$

The previous equations give a simple and fast algorithm to solve the problem and even to account for a slowly time-varying inlet mean flow velocity.